

A label-free and high-throughput separation of neuron and glial cells using an inertial microfluidic platform

Tiantian Jin,^{1,a)} Sheng Yan,^{2,a)} Jun Zhang,^{2,a)} Dan Yuan,²
 Xu-Feng Huang,^{1,b)} and Weihua Li^{2,b)}

¹*Centre for Translational Neuroscience, School of Medicine, University of Wollongong, and Illawarra Health and Medical Research Institute (IHMRI), Wollongong, New South Wales 2522, Australia*

²*School of Mechanical, Materials and Mechatronic Engineering University of Wollongong, Wollongong, New South Wales 2522, Australia*

(Received 9 March 2016; accepted 3 May 2016; published online 12 May 2016)

While neurons and glial cells both play significant roles in the development and therapy of schizophrenia, their specific contributions are difficult to differentiate because the methods used to separate neurons and glial cells are ineffective and inefficient. In this study, we reported a high-throughput microfluidic platform based on the inertial microfluidic technique to rapidly and continuously separate neurons and glial cells from dissected brain tissues. The optimal working condition for an inertial biochip was investigated and evaluated by measuring its separation under different flow rates. Purified and enriched neurons in a primary neuron culture were verified by confocal immunofluorescence imaging, and neurons performed neurite growth after separation, indicating the feasibility and biocompatibility of an inertial separation. Phencyclidine disturbed the neuroplasticity and neuron metabolism in the separated and the unseparated neurons, with no significant difference. Apart from isolating the neurons, purified and enriched viable glial cells were collected simultaneously. This work demonstrates that an inertial microchip can provide a label-free, high throughput, and harmless tool to separate neurological primary cells. *Published by AIP Publishing.* [<http://dx.doi.org/10.1063/1.4949770>]

I. INTRODUCTION

Schizophrenia is a globally challenging brain disorder that affects about 0.5%–1% of the general population.¹ People diagnosed with schizophrenia suffer from hallucinations, delusions, thought disorders, and cognitive deficits.² Previous neuropathological studies suggested that serious deficits in the neuronal processes and neuronal synaptic connectivity contribute to schizophrenia,³ which is why the role of neurons in brain regions is of high interest in investigating cognitive and affective impairments in schizophrenia. One huge challenge is to separate neurons from complex cell mixtures dissected from brain tissues because the primary neuron culture is a widely applied experimental method for isolating neurons that closely mimics the physiological status of neurons *in vivo*. However, the traditional method makes it difficult to distinguish neurons from glial cells that normally outnumber neurons in mammalian brain tissues.⁴

The traditional method for pure neuron and pure glial cell cultures is a medium-based procedure where a NeuroBasal medium with FDU (5-Fluoro-2'-deoxyuridine) to inhibit glial cells for long term incubation is widely used.^{5–7} However, this method needs long term incubation with chemical treatment, which is a huge waste of time and experimental materials. Meanwhile, Dulbecco's Modified Eagle's Medium (DMEM) is the most commonly used medium for glial cell culture or non-neuron cell culture.^{5,8,9} Some studies have suggested that

^{a)}T. Jin, S. Yan, and J. Zhang contributed equally to this work.

^{b)}Authors to whom correspondence should be addressed. Electronic addresses: weihuali@uow.edu.au and xhuang@uow.edu.au.

DMEM may also be suitable for primary neuron culture,¹⁰ and therefore separating neuron and glial cells by the traditional medium-based methods is difficult and inefficient.

Apart from medium-based separation methods, immune-specific separation is significant in neuron-related research. The fluorescence-activated cell sorting (FACS) and magnetically activated cell sorting (MACS) have been broadly applied in a biological laboratory for sorting cells.¹¹ However, labelling target cells requires several time consuming and labour intensive steps, and more importantly, applying antibodies to label cells for separation may further disturb the immunochemistry analysis on targets of interest. Microfluidic technology has increasingly become a versatile tool to control the neuronal microenvironment precisely whilst selectively probing for axons of neurons in a reproducible fashion.^{12–14} Dielectrophoresis (DEP) that distinguishes cells by their dielectric properties is a label-free technique for neuronal and glial cells separation. Prasad *et al.*¹⁵ presented a 4×4 micro-electrode array microchip to isolate and relocate individual neurons from hippocampal cells using DEP. Zhou *et al.*¹⁶ recently described the separation of embryonic mouse hippocampal neurons from a co-culture of glial cells using multi-electrode arrays, but these devices require a low conductivity DEP buffer, which is not bio-compatible. Furthermore, these devices normally run in a batch manner and with a very limited throughput. Apart from DEP, Wu *et al.*¹⁷ also reported on the application of viscoelasticity tuned hydrodynamic spreading on neural cell separation where the microfluidic device works in a continuous and label free manner. Their device could achieve high viability neural cell separation independent of medium dielectric properties. However, the flow rate (20 $\mu\text{L}/\text{h}$) and the throughput (3×10^4 cells/h) are still not satisfactory, and therefore need further improvement.

There is an urgent need for a high-throughput technique that can continuously separate neurons and glial cells in a culture medium to bridge this gap for neuroscience. Inertial microfluidics is a very promising candidate due to its high throughput and simple structure, as well as being independent of the conductivity of the medium, and compatible with the cell culture medium. It has been widely used to extract blood plasma,^{18,19} isolate circulating tumour cells (CTCs),^{20–22} and separate leukocytes from blood.²³

We therefore propose to use the inertial microfluidic technique to separate hypothalamic neurons and glial cells. Recent studies have revealed a hypothalamic structural abnormality and alternating neuropeptides in schizophrenia,^{24–26} indicating that the hypothalamus may have a role in schizophrenia pathology and treatment. Compared with conventional protocol that isolates hypothalamic neurons at the expense of the apoptosis of glial cells using specific chemicals, this inertial microchip can simultaneously collect purified viable neurons and glial cells in a label-free, rapid, and continuous fashion, which shortens and simplifies the cell preparation process.

II. METHODS AND MATERIALS

A. Overall workflow

Hypothalamic tissues were dissected from postnatal one day C57BL/6 mice ($n=6$). Brain tissues were then digested to collect cell suspensions that were then transferred into an inertial microchip for separation. Cell suspensions were collected from the outlet middle and outlet aside, respectively, and then immunostaining was performed to evaluate the separation performance. In addition, cells collected from the outlet middle were also plated into poly-D-lysine-coated coverslips in a 24-well plate in culture medium and maintained at 37 °C with 5% CO₂ (Fig. 1(a)).

B. Mechanism

The inertial separation of neuron and glial cells in a serpentine channel is based on our previous study regarding differential equilibrium positions in the serpentine channel for different sized micro-particles.²⁷ Three inertial effects (or forces) are exerted onto micro-particles flowing in a serpentine channel: the inertial lift forces, secondary flow drag, and centrifugal force.²⁸ When the medium density is very close to the particles, the effect of centrifugal force is

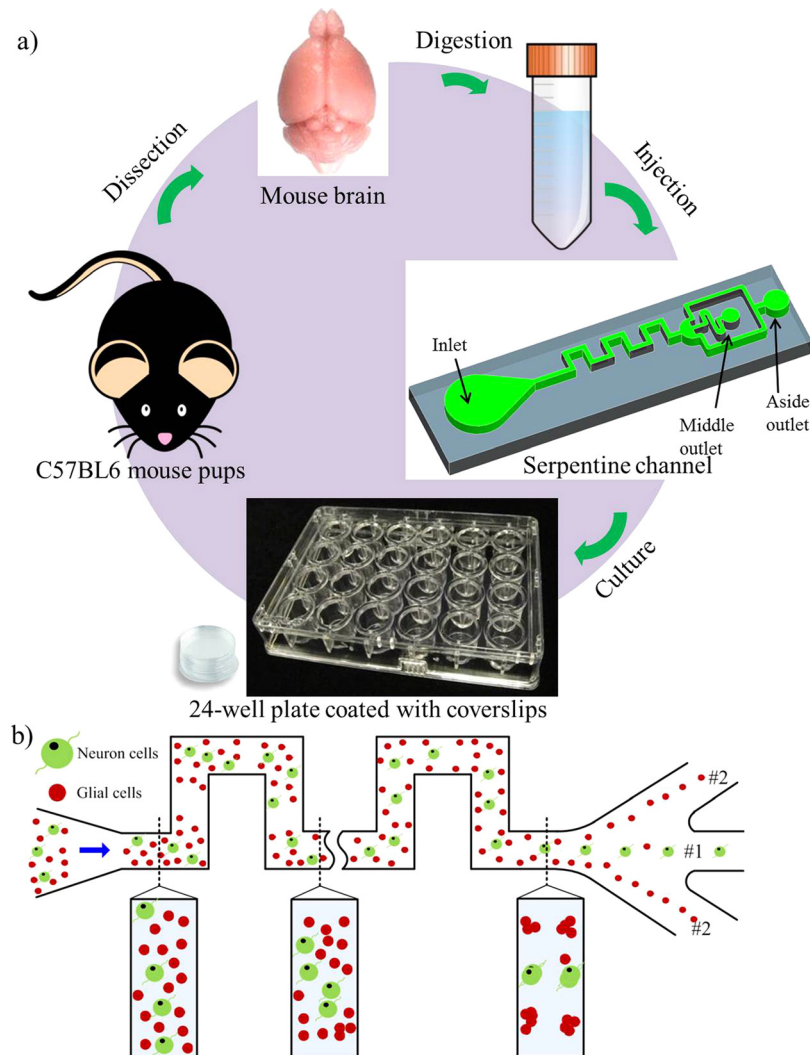


FIG. 1. (a) Overall workflow of the device, including the dissection of mouse pups, trypsinization of mouse brains, injection of cells into the inertial microchip, and culturing separated cells for various downstream immunostaining and PCP tests. (b) Schematics of inertial separation of neuron and glial cells in the inertial microchip with a symmetrical serpentine channel. Large neuron cells migrate into the outlet middle, while most of the smaller glial cells are collected in the outlet aside.

negligible because the inertial lift forces focus cells towards the two sidewalls, while secondary flow in the serpentine channel with alternating curvature pinches cells into the centre of the channel. Therefore, the final focusing position of cells is determined by the relative strength of the inertial lift forces and the secondary flow drag; large cells experiencing a much stronger secondary flow drag force are prone to migrate into the centre of the microchannel under a certain flow region, whilst small cells are mostly focused near the two sidewalls because they experience much stronger inertial lift forces than the secondary flow drag. A previous study based on human post mortem tissue indicated that the somas of neuronal cells are $4.7\text{--}22.4\text{ }\mu\text{m}$ in diameter, while the somas of glial cells are only $2.6\text{--}8.7\text{ }\mu\text{m}$ in diameter.²⁹ Although there is a size overlap ($4.7\text{--}8.7\text{ }\mu\text{m}$) between these two kinds of cells, there is a significant difference in size between neurons and glial cells, so by selecting a suitable flow condition, neuronal cells experience a dominant secondary flow drag and can be focused at the centre of the serpentine channel. Moreover, glial cells simultaneously experience a dominant inertial lift force and focus at the two sidewalls, and therefore neurons and glial cells can be separated efficiently by collecting the corresponding particle streams, as shown schematically in Fig. 1(b).

C. Design and fabrication

The serpentine channel used in our experiments consists of 15 zigzag periods; the channel has a uniform $42\ \mu\text{m}$ depth, and the length and width of each U-turn are $700\ \mu\text{m}$. The micro-channel is $200\ \mu\text{m}$ wide. A trifurcating outlet at the end of the channel is implemented at the end of the serpentine channel. Two-sided symmetrical bifurcations are combined into a single outlet to simplify the collection of two-sided streams. The microfluidic device was fabricated by the standard photolithography and soft lithography techniques.³⁰

D. Device preparation

Prior to these cell experiments, the device was rinsed with phosphate buffered saline (PBS) at $100\ \mu\text{l}/\text{min}$ for 10 min using a syringe pump (Legato 100, Kd Scientific), after which the devices were sterilised through exposure to UV light for 30 min.

E. Cell separation

Hypothalamic cell cultures were prepared according to previous literature and protocols,^{5,6} and hypothalamic sections were dissected from postnatal one day C57BL/6 mice. Hypothalamic tissues were digested and triturated to suspend cells in 7 ml culture medium. A 2 ml cell suspension was kept as an inlet group for comparison, while the other 5 ml hypothalamic cell suspension was infused into the inertial microchip to perform separations under different flow rates. Separated cells were collected from the outlet middle and outlet aside, respectively, under three typical flow rates to compare the separation performance. After determining the optimal flow rate, cells separated from the optimal flow rate were used for further culture and tests. To evaluate separation performance, the purity of separation and the enrichment ratio were measured. Separation purity is defined as the ratio of the number of target cells to the total number of cells, while enrichment is defined as the concentration ratio between the target cells from the outlet to the target cells from the inlet.

F. Mouse hypothalamic neuron culture

A culture medium was modified for neuron incubation based on the Johns Hopkins online protocol;⁶ this culture medium generally consists of a NeuroBasal medium with an additive B27 and extra glucose and glutamine. Cells from inlet and outlet middle were plated into poly-D-lysine (P6407, Sigma-Aldrich) coated coverslips in a 24-well plate and maintained at 37°C with 5% CO_2 . To examine their rate of growth, neurons were collected after 10 days of incubation (DIV 10) for immunofluorescence and image analysis. To determine how well the cell responded to phencyclidine (PCP) stimulations, neurons at DIV 10 were administered with $25\ \mu\text{M}$ PCP (P3209, Sigma-Aldrich) for 3 h and 48 h and were then collected for immunofluorescence and image analysis.

G. Immunofluorescence and image analysis

For immunofluorescence staining, cells from the outlet middle and outlet aside, as well as further cultured neurons from the outlet middle, were fixed with 4% paraformaldehyde in Dulbecco's PBS for 30 min at room temperature. These samples were further incubated with 100% methanol for 20 min at -20°C and then blocked with 5% goat serum in PBS for 1 h at 37°C , and then anti-NeuN antibody (MAB377, Merck Millipore), anti-microtubule-associated protein 2 (MAP2) antibody (M9942, Sigma-Aldrich), anti-glial fibrillary acidic protein (GFAP) antibody (G9269, Sigma-Aldrich), and anti-brain derived neurotrophic factor (BDNF) antibody (SC-20981, Santa-cruz) were applied overnight at 4°C . GFAP and BDNF were visualised with isotype-specific goat anti-rabbit IgG (H+L) secondary antibody conjugated with Alexa Fluor 488 (A11008, ThermoFisher). NeuN and MAP2 were visualised by goat anti-mouse IgG (H+L) secondary antibody conjugated to Alexa Fluor 594 (A11004, ThermoFisher). The concentrations of antibodies were applied according to the manufacturers' manuals. A confocal

microscope (Leica TCS SP5 Advanced System, Leica Microsystems) was used to obtain fluorescent images of the stained cells, while software Image J with plugin NeuriteQuant³¹ was used to quantify the immunoreactivity.

H. Statistical analysis

Data were analysed using the SPSS statistical package (SPSS.19, IBM). A two-tailed *t* test was applied to analyse the separation of different flow rates, variations in cell concentration between the inlet, outlet middle, and outlet aside, neuron enrichment and neuron purity from the outlet middle, glial cell enrichment and glial cell purity from the outlet aside, and neurite length and neurite branches. A one way analysis of variance (ANOVA) and the *post-hoc* Tukey-Kramer honestly significant difference (HSD) test were used to study the response of neurons to PCP stimulations. A *p* value <0.05 was regarded as statistically significant. The values in Fig. 2 were expressed as mean \pm SD, and the values in Figs. 3–5 were showed as mean \pm SEM.

III. RESULTS

A. The effect of flow rates on size-based cell separation

A digested cell suspension was processed under three typical flow conditions to investigate how the flow rates affected the separation. The unprocessed cell suspension was taken as an inlet (control) group. Cells from the inlet group and two outlet groups were counted in a hemocytometer and their sizes were measured. Since the inlet group contained neuronal and glial cells, the cell size distribution was quite broad. The average cell size was $7.4\ \mu\text{m}$, with a standard deviation of $3.2\ \mu\text{m}$ (Table I). Fig. 2(a) and Table I show that most neuronal (MM) and glial cells (MA) could be separated according to their size under a flow rate of $550\ \mu\text{l/min}$, a flow condition in which a distinct size threshold of $\sim 6\ \mu\text{m}$ could be interpreted. Cells that were above this threshold were prone to be collected by the outlet middle collection (Fig. 2(a), MM); their average size was $9.9 \pm 1.8\ \mu\text{m}$ (Table I). Cells below this threshold were mostly collected from the outlet aside (Fig. 2(b), MA), and they had mean sizes of $4.6 \pm 1.0\ \mu\text{m}$ (Table I). Note that a tiny part of the small cells was still inevitably collected in the outlet middle collection, indicating the possible existence of glial cells. Although a perfectly pure collection of neurons cannot be expected via this inertial microchip, a much purer neuron cell suspension could be achieved, with most glial cells depleted.

However, for the high flow rate of $750\ \mu\text{l/min}$, even though there was a distinct threshold for cell separation according to Fig. 2(a), the cell size distribution from middle collection (HM) was rather large ($8.9 \pm 2.5\ \mu\text{m}$; Table I), indicating that more glial cells had been collected under this condition (Fig. 2(b)). Small cells tended to become defocused due to the mixing effects of secondary flow under such a high flow speed and were distributed almost uniformly along the width of the channel, and therefore a large part of glial cells were collected by the outlet middle. At a low flow rate of $350\ \mu\text{l/min}$, the cells could not be separated according to the size because the large and small cells were both focused along two sides of the channel and collected by the outlet aside (Fig. 2, Table I, LA). Cells collected by the outlet middle were those that had randomly escaped from the cell focusing streaks (Fig. 2, LM). Based on these results, a moderate flow rate of $550\ \mu\text{l/min}$ was chosen to separate the neuronal and glial cells in the following tests. Cell suspensions were collected to perform immunofluorescence staining to confirm the separation effect and then incubated for 10 days to examine neuron growth and response to PCP stimulations.

B. Enriched and purified neurons and glial cells by inertial separation

Our optimization experiments suggested that a moderate flow rate ($550\ \mu\text{l/min}$) was the optimal working condition for separating cells, but for further confirmation, equal volumes (1 ml) of cells were collected from the inlet, outlet middle, and outlet aside for immunostaining immediately after separation. An anti-NeuN antibody was applied to detect neurons and an

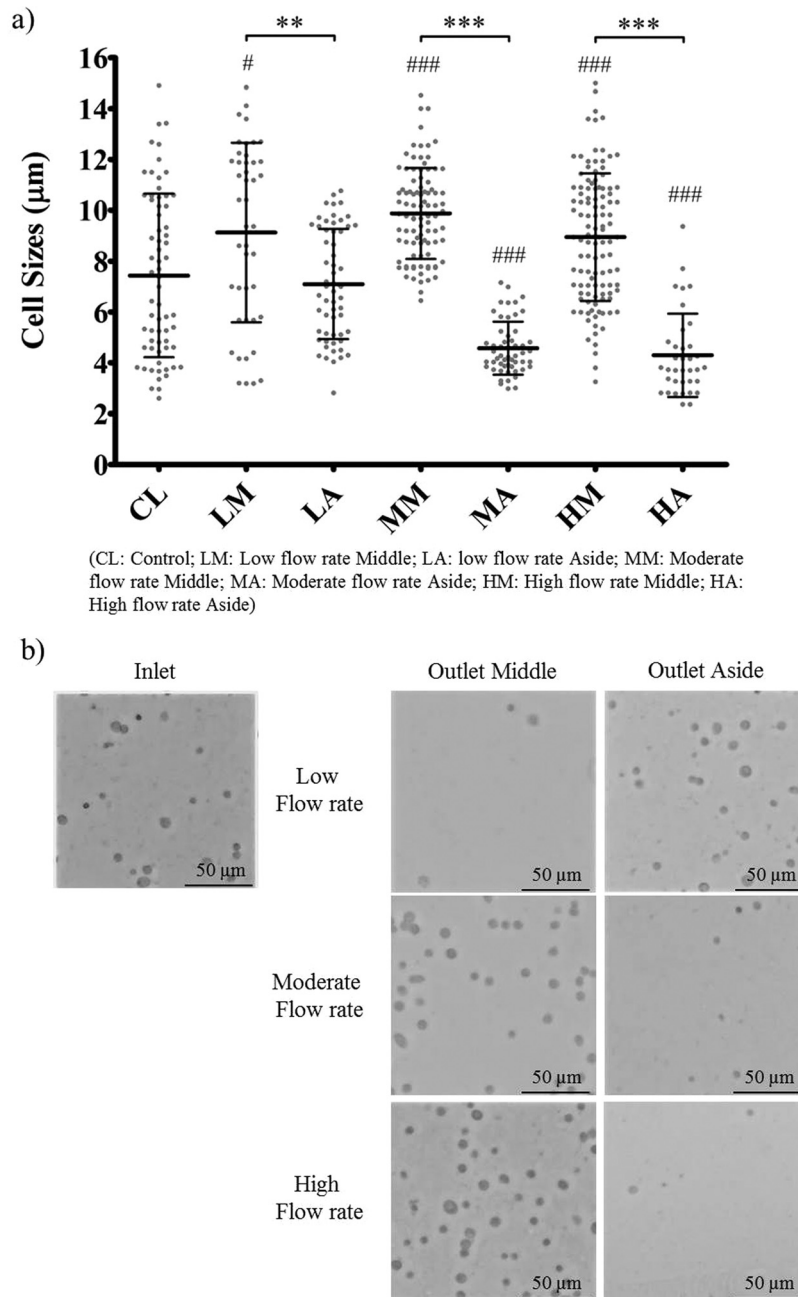


FIG. 2. Separation of neuronal and glial cells by an inertial microchip under three typical flow rates. (a) Size distribution of cells from inlet (control, CL), and two collections from outlet middle (LM, MM, and HM) and outlet aside (LA, MA, and HA) under three typical flow conditions. The first letter L, M, and H mean three different flow rates L (low, $350 \mu\text{l/min}$), M (moderate, $550 \mu\text{l/min}$), and H (high, $750 \mu\text{l/min}$). The second letter M and A indicates collection positions middle and aside, respectively. Data represent mean \pm SD ($n=5$). A two-tailed t test was applied. # $p < 0.05$, ### $p < 0.001$ represented outlet groups versus control group; ** $p < 0.01$, *** $p < 0.001$ was used between the outlet middle and outlet aside in each flow rate group. (b) Images of cells from the inlet (control, CL), and two collections from the outlet middle and outlet aside under the three flow conditions.

anti-GFAP antibody was applied to stain astrocytes, which is the major cell type of glial cells. The immunofluorescence results confirmed that most cells in outlet middle were neurons (Fig. 3(a)), with a purity as high as $92 \pm 1.5\%$; this was much higher than the $58 \pm 5.4\%$ in the inlet (Fig. 3(b)). In addition, the glial cells increased in purity from $36 \pm 5.2\%$ in the inlet to $81 \pm 1.4\%$ in the outlet aside (Fig. 3(c)), indicating much purer neuron and glial cells.

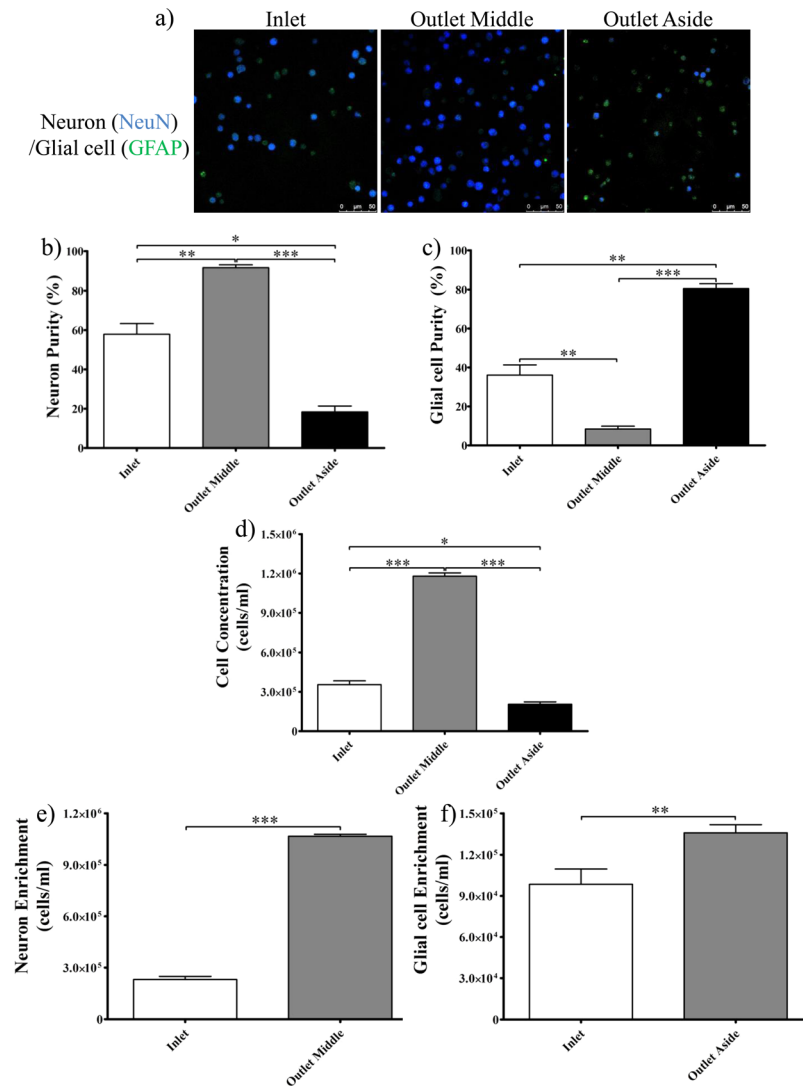


FIG. 3. Inertial separation of neuronal and glial cells at the optimal flow condition ($550 \mu\text{l}/\text{min}$). (a) Cells collected from the inlet, outlet middle, and outlet aside were stained by neuron marker NeuN (blue) and astrocyte marker GFAP (green) after separation. (b) Purity of neuronal cells in the inlet (control), outlet middle, and outlet aside. (c) Purity of glial cells in the inlet (control), outlet middle, and outlet aside. (d) Concentrations of cells in the inlet, outlet middle, and outlet aside. (e) Enrichment of concentrated neurons in the outlet middle. (f) Enrichment of glial cell astrocytes in the outlet aside. Data represent mean \pm SEM ($n=5$, obtained from 5 independent cultures). A two-tailed t test was applied. * $p < 0.05$, ** $p < 0.01$, *** $p < 0.001$.

Furthermore, the results showed a high level of total cell concentration (1.2×10^6 cells/ml) in the outlet middle; this is a 3.3-fold increase compared to a cell concentration of (3.6×10^5 cells/ml) in the inlet (Fig. 3(d), indicating cell enrichment by separation. Considering the enhanced purity of neurons from the inlet to outlet middle, neurons were enriched from 2.3×10^5 cells/ml in the inlet to 1.07×10^6 cells/ml in the outlet middle (Fig. 3(e)). For glial cells, although the total cell concentration in the outlet aside (2.1×10^5 cells/ml) is lower than the inlet (Fig. 3(d)), the glial cell astrocytes were still enriched from 9.8×10^4 cells/ml (inlet) to 1.36×10^5 cells/ml (outlet aside) due to higher purity in the outlet aside (Fig. 3(f)).

C. Influence of inertial separation on neuron growth

The features of neurons are the growth of neurites and synaptogenesis. After microfluidic separation under a moderate flow rate, equal volumes (1 ml) of cells from the inlet (control)

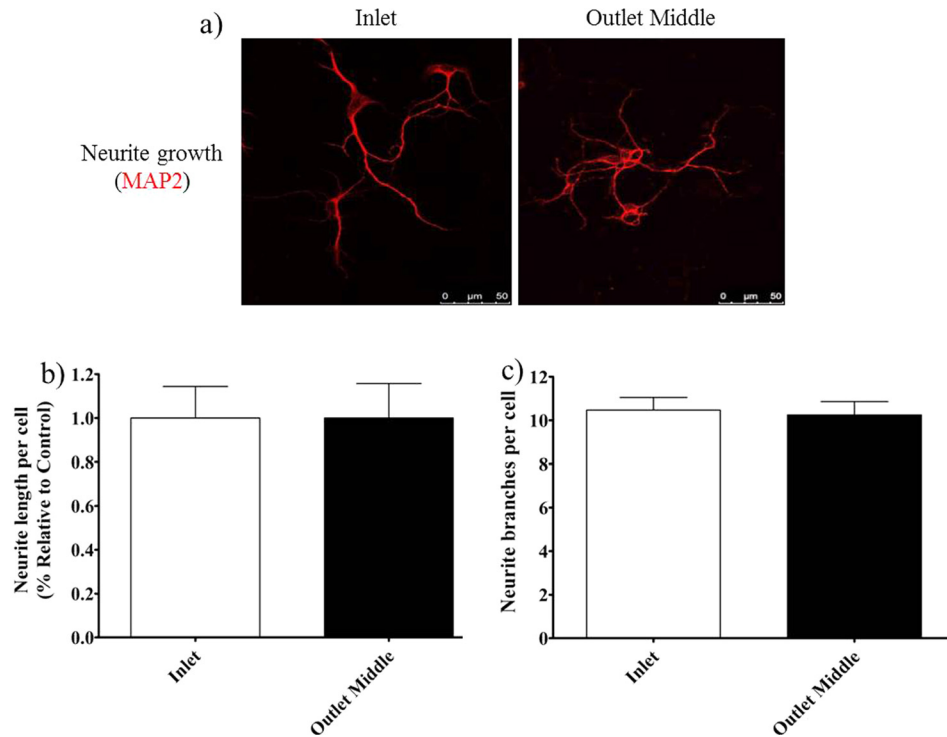


FIG. 4. Neurite growth of neuronal cells in the inlet (unprocessed) and outlet middle after inertial separation. (a) Fluorescent images of neurite growth of neurons in the inlet and outlet middle after inertial separation. Neurons collected from the inlet and outlet middle were stained by structural protein marker MAP2 (red) to label neurite synapses and dendrites. (b–c) There is no difference in the length and branches of neurites per cell in the inlet and outlet middle groups. Data represent the mean \pm SEM ($n=5$, obtained from 5 independent cultures). A two-tailed t test was applied, and there was no statistical difference between the two groups.

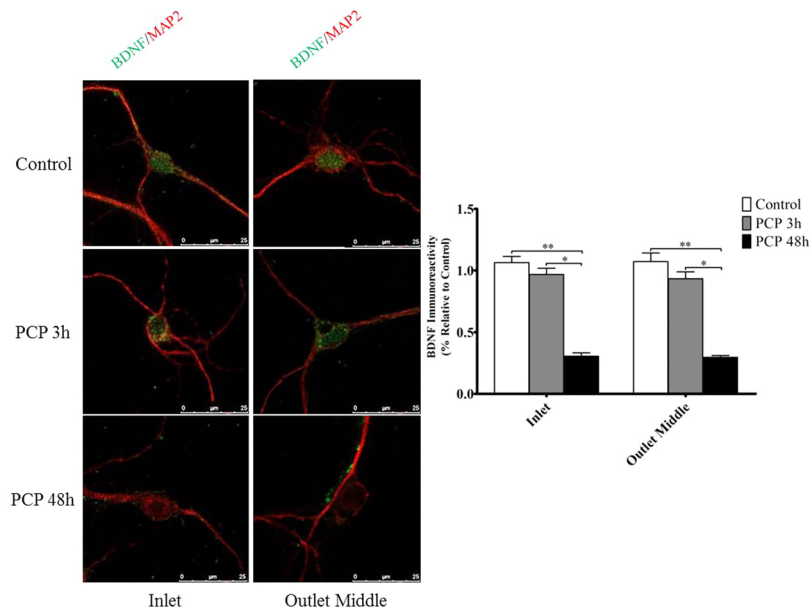


FIG. 5. BDNF expressions were inhibited in neurons from the inlet and outlet middle after treatment with PCP. There are no differences in the responses to PCP stimulations for neurons at the inlet and outlet middle. Data represent mean \pm SEM ($n=5$, obtained from 5 independent cultures). Significance was calculated by ANOVA and the *post-hoc* Tukey-Kramer HSD test. * $p < 0.05$, ** $p < 0.01$ versus control (without PCP).

TABLE I. List of cells' average size and standard deviation from the inlet (control) and two outlets under three different flow rates (LM: low flow rate middle; LA: low flow rate aside; MM: moderate flow rate middle; MA: moderate flow rate aside; HM: high flow rate middle; HA: high flow rate aside).

	CL	LM	LA	MM	MA	HM	HA
Mean (μm)	7.4	9.1	7.1	9.9	4.6	8.9	4.3
SD (μm)	3.2	3.5	2.2	1.8	1.0	2.5	1.7

and outlet middle were collected and incubated to investigate how inertial separation affected the growth of neurons. Since MAP2 is a neuron-specific cytoskeletal protein that can be stained to detect neuron soma, synapses, and dendrites, MAP2 antibody immunostaining was applied to the inlet group and outlet middle group at DIV 10 to characterise neuron morphology. Image J with plugin NeuriteQuant³¹ was used to examine the growth and synaptogenesis of neurite by calculating its length and branches. The results confirmed that neurons from both groups generated the same neurite growth (Fig. 4(a)), and there was no statistical difference between the two groups in the length of neurites per cell (Fig. 4(b)) and their branches per cell (Fig. 4(c)). Therefore, the inertial separation of neuron cells does not have a negative influence on the growth of neurons.

D. Influence of inertial separation on the response of neurons to PCP stimulations

To demonstrate that neurons separated from the inertial microchip could be an ideal platform for further biological studies, cells from the inlet (control) and outlet middle at DIV 10 were exposed to PCP for acute stimulations for 3 h and chronic stimulations for 48 h, respectively. PCP has been studied extensively for decades because it can mimic symptoms in patients diagnosed with schizophrenia. Previous research has confirmed that PCP can impact on the metabolism and neurochemistry of the brain regions in a time manner.³² Immunostaining was applied to detect the expression of BDNF, an important neurotrophic factor for neuroplasticity and neuron metabolism. In the outlet middle neurons, BDNF expression decreased partly in acute treatment and then significantly reduced during chronic treatment (Fig. 5). The same results were also observed in the inlet neurons, which means that separation did not have a negative effect on the biological response of neurons to PCP stimulations; it further proves that the inertial device did not harm the neuron cells and the processed neuronal cells were healthy and functional. The total residual time of individual neurons in the serpentine channel of inertial microchip was estimated to be 15 ms, which shortened the time that neurons were exposed to shear stress, and may be why there is no negative influence on the biophysical characteristics of separated neurons for protein expressions.

IV. DISCUSSION

Here, we developed a modified protocol using an inertial microchip to continuously separate neurons and glial cells. This proposed microfluidic platform was based on size-dependent separation. Cells collected from the outlet middle of the micro-channel were characterised as large cells (Fig. 2) with increased concentration, and we confirmed that these large cells were neurons by immunostaining (Fig. 3(a)), and therefore plated neurons from the outlet middle were enriched and purified (Figs. 3(b) and 3(e)). In the traditional medium-based method, neurons are mixed with glial cells where neurons with a low purity are used for incubation and further experiments. Our proposed method makes the primary cell culture more efficient by collecting more purified neuron samples at once, while the device can process 5 ml of cell suspension within 10 min, thus speeding up the preparation of samples. In addition, our method avoids using extra brain tissues and culture mediums that not only saves many samples but also meets the requirement of animal ethics, which suggests a minimal number of animals to be sacrificed. Moreover, separated neurons were as healthy and functional as unprocessed ones, and

there was no significant variation of in the growth and synaptogenesis of neurite caused by the inertial separation procedure (Fig. 4). Moreover, the PCP treatment of unprocessed cells from the inlet and processed cells from the outlet middle displayed the same biological responses, thus demonstrating the biocompatibility of the separation procedure. The continuity of cell separation and short residual time in the channel minimised any unexpected shear-induced effects to the neuronal phenotype. This is critical for the subsequent molecular characterisation of biological functions or gene expression of specific drug therapy. Therefore, this platform is a robust, efficient, and harmless tool for separating primary neuron cells.

Inertial separation is very important for future research into schizophrenia because applying an inertial microchip helps to separate neurons and isolate glial cells. As mentioned above, most cells from the outlet aside were small in size (Fig. 2), and further staining experiments indicated that they were mainly enriched and purified astrocyte type glial cells (Figs. 3(c) and 3(f)). Astrocytes were only examined by staining with anti-GFAP antibody because astrocyte is the major component of glial cells, although there was around 5% of unstained glial cells, including microglia and oligodendrocyte. Note also that the total number of glial cells was less than the number of neurons in the inlet sample because the mice pups were sacrificed in postnatal day 1 to ensure the health and activity of neurons. Meanwhile, the glia/neuron ratio was low in the first postnatal week, but it will increase significantly during the second and third postnatal weeks.³³ A new perspective has recently appeared suggesting that the dysfunction of glial cells due to astrocyte is also involved in the neuropathology of schizophrenia,³⁴ because it is the most numerous source of glial cells in mammalian brains. Various reports have revealed that altered density and genes due to expressions of astrocytes are strongly related to schizophrenia.³⁴ For example, astrocyte has a protein called S100B, of which there is a significant amount in schizophrenia patients,³⁵ which makes astrocyte a promising biomarker to predict first episode schizophrenia in the future.³⁶ Therefore, glial cells have become a major source to supply pathophysiological significance and possible therapeutic target. To investigate the individual contributions made by glial cells in the mechanism and treatment of schizophrenia, our advanced inertial microchip is a promising candidate for isolating glial cells from primary cell cultures.

Furthermore, the current microfluidic approaches for separating neurons and glial cells are mostly based on DEP, where cells of interest are trapped at the micro-electrodes in DEP devices, whereas the inertial microchip here can separate neurons and glial cells in a continuous manner. Compared to the fluid velocity of DEP device ($< 10 \mu\text{m/s}$),¹⁶ cells passed through the microchannel in the inertial microchip at $\sim 1 \text{ m/s}$, which significantly increased the processing speed and throughput. The throughput of our inertial microchip is 1.188×10^7 cells/h, which is a significant improvement compared to using viscoelasticity tuned hydrodynamic spreading.¹⁷ Although the throughput of the inertial chip is slower than the FACS, the throughput capability of our proposed device can be dramatically amplified by parallelizing several microchannels in the same microchip.¹⁹ Compared to FACS, our inertial device is label-free, which may significantly reduce the total processing time and costs.

V. CONCLUSIONS

In this work, we have demonstrated continuous, high purity, and harmless neuronal cell separation with an inertial microchip. This inertial microchip can enrich and purify primary neuronal cells with unaltered morphology and biological function, while simultaneously purifying and enriching glial cells. We therefore anticipate that this inertial microchip will be an outstanding plugin to advance the current primary cell separation and culture method for neuroscience.

ACKNOWLEDGMENTS

This work was supported by the University of Wollongong-China Scholarship Council joint scholarships. W.L., X.-F.H., T.J., S.Y., and J.Z. designed research. T.J., J.Z., S.Y., and D.Y. conducted experiments and analysed the data. T.J., S.Y., and J.Z. wrote the manuscript. All the authors have reviewed the manuscript. Mr. Robert Clayton, Mr. Tanju Yildirim, and the anonymous reviewers helped to polish English.

- ¹R. Freedman, *New Engl. J. Med.* **349**(18), 1738–1749 (2003).
- ²C. A. Ross, R. L. Margolis, S. A. J. Reading, M. Pletnikov, and J. T. Coyle, *Neuron* **52**(1), 139–153 (2006).
- ³P. J. Harrison and S. L. Eastwood, *Hippocampus* **11**(5), 508–519 (2001).
- ⁴B. Connors, M. F. Bear, and M. Paradiso, *Neuroscience—Exploring the Brain*, 3rd ed. (Lippincott Williams & Wilkins, Philadelphia, 2006).
- ⁵L. G. W. Hilgenberg and M. A. Smith, *J. Vis. Exp.* **10**, 562 (2007).
- ⁶Johns Hopkins Medicine, *Dissociated Primary Hypothalamic Neuron Culture* (2015), see http://www.hopkinsmedicine.org/institute_basic_biomedical_sciences/research_centers/metabolism_obesity_research/protocols/.
- ⁷G. J. Brewer, *J. Neurosci. Methods* **71**(2), 143–155 (1997).
- ⁸J. Saura, *J. Neuroinflamm.* **4**, 26–26 (2007).
- ⁹S. Schildge, C. Bohrer, K. Beck, and C. Schachtrup, *J. Vis. Exp.* **71**, e50079 (2013).
- ¹⁰B. A. Barres, *Cold Spring Harb. Protoc.* **2014**(12), 1342–1347.
- ¹¹A. Radbruch and D. Recktenwald, *Curr. Opin. Immunol.* **7**(2), 270–273 (1995).
- ¹²G. M. Whitesides, *Nature* **442**(7101), 368–373 (2006).
- ¹³S. Takayama, E. Ostuni, P. LeDuc, K. Naruse, D. E. Ingber, and G. M. Whitesides, *Chem. Biol.* **10**(2), 123–130 (2003).
- ¹⁴S. Rhee, A. Taylor, D. Cribbs, C. Cotman, and N. Jeon, *Biomed. Microdevices* **9**(1), 15–23 (2007).
- ¹⁵S. Prasad, X. Zhang, M. Yang, Y. Ni, V. Parpura, C. S. Ozkan, and M. Ozkan, *J. Neurosci. Methods* **135**(1–2), 79–88 (2004).
- ¹⁶T. Zhou, S. F. Perry, Y. Ming, S. Petryna, V. Fluck, and S. Tatic-Lucic, *Biomed. Microdevices* **17**(3), 1–14 (2015).
- ¹⁷Z. Wu, K. Hjort, G. Wicher, and Å. Fex Svenningsen, *Biomed. Microdevices* **10**(5), 631–638 (2008).
- ¹⁸M. G. Lee, S. Choi, H. J. Kim, H. K. Lim, J. H. Kim, N. Huh, and J. K. Park, *Appl. Phys. Lett.* **98**(25), 253702 (2011).
- ¹⁹J. Zhang, S. Yan, W. Li, G. Alici, and N.-T. Nguyen, *RSC Adv.* **4**(63), 33149–33159 (2014).
- ²⁰A. J. Mach, J. H. Kim, A. Arshi, S. C. Hur, and D. Di Carlo, *Lab Chip* **11**(17), 2827–2834 (2011).
- ²¹H. W. Hou, M. E. Warkiani, B. L. Khoo, Z. R. Li, R. A. Soo, D. S.-W. Tan, W.-T. Lim, J. Han, A. A. S. Bhagat, and C. T. Lim, *Sci. Rep.* **3**, 1259 (2013).
- ²²E. Ozkumur, A. M. Shah, J. C. Ciciliano, B. L. Emmink, D. T. Miyamoto, E. Brachtel, M. Yu, P.-I. Chen, B. Morgan, and J. Trautwein, *Sci. Transl. Med.* **5**(179), 179ra147 (2013).
- ²³L. Wu, G. Guan, H. W. Hou, A. A. S. Bhagat, and J. Han, *Anal. Chem.* **84**(21), 9324–9331 (2012).
- ²⁴D. Fannon, L. Tennakoon, A. Sumich, S. O’Ceallaigh, V. Doku, X. Chitnis, J. Lowe, W. Soni, and T. Sharma, *Brit. J. Psychiatr.* **177**, 354–359 (2000).
- ²⁵E. Walker, V. Mittal, and K. Tessner, *Annu. Rev. Clin. Psychol.* **4**, 189–216 (2008).
- ²⁶H. Bernstein, H. Dobrowolny, and B. Bogerts, *Neuropeptide Res. Trends* 213–227 (2007).
- ²⁷J. Zhang, S. Yan, R. Sluyter, W. Li, G. Alici, and N.-T. Nguyen, *Sci. Rep.* **4**, 4527 (2014).
- ²⁸J. Zhang, W. Li, M. Li, G. Alici, and N.-T. Nguyen, *Microfluid. Nanofluid.* **17**(2), 305–316 (2014).
- ²⁹G. Rajkowska, L. D. Selemon, and P. S. Goldman-Rakic, *Arch. Gen. Psychiatry* **55**(3), 215–224 (1998).
- ³⁰D. C. Duffy, J. C. McDonald, O. J. A. Schueller, and G. M. Whitesides, *Anal. Chem.* **70**(23), 4974–4984 (1998).
- ³¹L. Dehmelt, G. Poplawski, E. Hwang, and S. Halpain, *BMC Neurosci.* **12**(1), 1–14 (2011).
- ³²B. J. Morris, S. M. Cochran, and J. A. Pratt, *Curr. Opin. Pharmacol.* **5**(1), 101–106 (2005).
- ³³F. Bandeira, R. Lent, and S. Herculano-Houzel, *Proc. Natl. Acad. Sci. U.S.A.* **106**(33), 14108–14113 (2009).
- ³⁴H.-G. Bernstein, J. Steiner, and B. Bogerts, *Expert Rev. Neurother.* **9**(7), 1059–1071 (2009).
- ³⁵M. Rothermundt, P. Falkai, G. Ponath, S. Abel, H. Burkle, M. Diedrich, G. Hetzel, M. Peters, A. Siegmund, A. Pedersen, W. Maier, J. Schramm, T. Suslow, P. Ohrmann, and V. Arolt, *Mol. Psychiatr.* **9**(10), 897–899 (2004).
- ³⁶S. Yelmo-Cruz, A. L. Morera-Fumero, and P. Abreu-Gonzalez, *Psychiatry Clin. Neurosci.* **67**(2), 67–75 (2013).